



Escola Tècnica Superior d'Enginyeries  
Industrial i Aeronàutica de Terrassa

UNIVERSITAT POLITÈCNICA DE CATALUNYA

Degree:

Aerospace Vehicles Engineering

Author:

Jonatan Domènech Arboleda

Title of the study:

Feasibility study of the use of Rapid Manufacturing  
Technology in a new Unmanned Air Vehicle design

Directors:

Pau Nualart Nieto

Dra. Jasmina Casals Terré

Delivery date:

June 25<sup>th</sup>, 2014

Contents:

**6<sup>th</sup> DOCUMENT ANNEX IV: 3D PRINTING TESTS**

---

## Contents

<b>1</b>	<b>LIST OF FIGURES.....</b>	<b>3</b>
<b>2</b>	<b>LIST OF TABLES.....</b>	<b>3</b>
<b>3</b>	<b>NOMENCLATURE .....</b>	<b>4</b>
<b>4</b>	<b>INTRODUCTION.....</b>	<b>5</b>
<b>5</b>	<b>3D PRINTING TECHNOLOGY .....</b>	<b>6</b>
<b>6</b>	<b>MATERIAL .....</b>	<b>7</b>
6.1	ABS .....	7
6.2	PLA.....	7
6.3	NYLON .....	8
6.4	Material selection.....	8
6.5	PLA tensile test.....	11
<b>7</b>	<b>REPRAP 3D PRINTER ANALYSIS.....</b>	<b>16</b>
7.1	STL exportation .....	16
7.2	G-Code programming .....	17
7.3	Linear model approximation .....	21
7.4	Nonsupport material .....	29
7.5	Printing time and cost estimation.....	30
7.6	Help & support community .....	30
<b>8</b>	<b>PRINTING TEST.....</b>	<b>32</b>
8.1	Start printing calibration and bed fixation .....	33
8.2	Fluid mechanics analysis.....	33
8.3	TREE method .....	36
8.4	CHEDDAR method.....	38
8.5	CLICK method .....	40
8.6	STOP PRINTING method.....	41

8.7	Lattice 3D honeycomb.....	42
8.8	Airfoil.....	43
8.9	Maximum Z axis printing.....	44
<b>9</b>	<b>CONCLUSIONS.....</b>	<b>45</b>
<b>4</b>	<b>REFERENCES.....</b>	<b>46</b>

## 1 LIST OF FIGURES

FIGURE 1: REPRAP BCN 3D+ [1].....	6
FIGURE 2: AVAILABLE FILAMENT ABS-PLA-NYLON WEIGHT TEST.....	9
FIGURE 3: MD SAMPLE G-CODE.....	12
FIGURE 4: PLA 3D PRINTED MD SAMPLE .....	12
FIGURE 5: TD SAMPLE G-CODE.....	13
FIGURE 6: PLA 3D PRINTED TD SAMPLE .....	13
FIGURE 7: PLA TENSILE TEST GRAPHIC.....	14
FIGURE 8: STL EXPORTING COMMAND .....	16
FIGURE 9: SLIC3R PRINTER SETTINGS.....	18
FIGURE 10: SLIC3R FILAMENT SETTINGS.....	18
FIGURE 11: SLIC3R LAYERS AND PERIMETERS.....	19
FIGURE 12: SLIC3R INFILL .....	19
FIGURE 13: SLIC3R INFILL PATTERNS AND DENSITY MATRIX [13] .....	20
FIGURE 14: SAMPLES MATRIX.....	23
FIGURE 15: (0.25, 60) AND (0.10, 90) SAMPLE SURFACES.....	23
FIGURE 16: RESTS (E) VERSUS AVERAGE Y.....	29
FIGURE 17: RED EYED TREE FROG PRINTING TEST .....	32
FIGURE 18: PLA 400 MM THREAD.....	33
FIGURE 19: 3D PRINTING PROCESS SKETCH .....	35
FIGURE 20: ANGLE TESTER MODEL.....	36
FIGURE 21: MAXIMUM TREE ANGLE TEST .....	37
FIGURE 22: TREE MAXIMUM DEGREE COLLAPSE .....	38
FIGURE 23: CHEDDAR CAD DESIGN.....	39
FIGURE 24: CHEDDAR TRIGONOMETRIC RELATIONSHIP .....	39
FIGURE 25: AILERON CLICK METHOD TESTING MODEL.....	40
FIGURE 26: ELEVATOR G-CODE LAYERS SIMULATION.....	41
FIGURE 27: LATTICE 3D HONEYCOMB.....	43
FIGURE 28: AIRFOIL TEST 3D PRINTING .....	43
FIGURE 29: 200MM Z AXIS TEST .....	44

## 2 LIST OF TABLES

TABLE 1: REPRAP BCN 3D+ PRINTING FEATURES [1] .....	6
TABLE 2: ALTERNATIVES SPECIFICATIONS [6].....	9
TABLE 3: MATERIAL SELECTION SCORES TABLE .....	10

TABLE 4: MATERIAL SELECTION APPRECIATION MATRIX .....	10
TABLE 5: MATERIAL SELECTION DOMINATION MATRIX.....	10
TABLE 6: MATERIAL SELECTION RESULT.....	10
TABLE 7: PLA TENSILE TEST RESULTS.....	14
TABLE 8: WEIGHT MEASUREMENTS OF THE LINEAR MODEL EXPERIMENTATION.....	22
TABLE 9: LINEAR MODEL ESTIMATED ERROR.....	25
TABLE 10: B <sub>j</sub> TYPE ERRORS.....	26
TABLE 11: FIRST LINEAR MODEL ANOVA.....	26
TABLE 12: FIRST LINEAR MODEL COEFFICIENTS SIGNIFICANCE.....	26
TABLE 13: SECOND LINEAR MODEL ANOVA.....	27
TABLE 14: SECOND LINEAR MODEL COEFFICIENTS SIGNIFICANCE.....	27
TABLE 15: THIRD LINEAR MODEL ANOVA .....	28
TABLE 16: THIRD LINEAR MODEL COEFFICIENTS SIGNIFICANCE .....	28
TABLE 17: THIRD LINEAR MODEL ANOVA .....	28

### 3 NOMENCLATURE

UAV	Unmanned Air Vehicle
RMS	Rapid Manufacturing System
SLS	Selective Laser Sintering
DMLS	Direct Metal Laser Sintering
FDM	Fused Deposition Modeling
SLA	Stereo-lithography
LOM	Laminated Object Manufacturing
EBM	Electron Beam Melting
PP	Plaster-Based 3D Printing
CAD	Computer-aided Design
CNC	Computer Numeric Control
STL	STereoLithography file format
PA	Nylon
PLA	PolyLactic Acid
NIST	National Institute of Standards and Technology
ABS	Acrylonitrile butadiene styrene
MD	Machine Direction
TD	Transverse Direction
NIST	National Institute of Standards and Technology

## 4 INTRODUCTION

The aim of this document is to learn how to use 3D printing technology for the next applications in UAV. The goal is to learn the RepRap's features and to select the material for this study.

The selected material, biodegradable PLA, has been evaluated after the printing machining. This has allowed this study to know the mechanical properties of 3D printed PLA.

RepRap 3D printer has been analyzed in order to know how to use it and how to configure the parameters to specify the lightweight requirements of UAV application.

Printing test stage has become into the development of a useful methodology for 3D printing design with: TREE, CHEDDAR, CLICK and STOP PRINTING methods.

Finally this technology has been tested in UAV applications such as wing parts and infill methodology development with the 3D lattice honeycomb.

## 5 3D PRINTING TECHNOLOGY

The selected 3D printing device has been the RepRap<sup>1</sup> BCN 3D+ [1], see Figure 1, a self-replicating printer and OPEN SOURCE made in Barcelona for the Fundació CIM<sup>2</sup>.

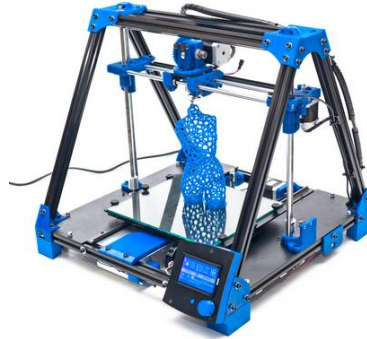


Figure 1: RepRap BCN 3D+ [1]

RepRap BCN 3D+ basic features has been enumerated, see Table 1. This information shows the Open Source philosophy, the low cost device, the close support service, the high speed performance and the accuracy, the big printing volume and the multi-material availability, see attachment: ANNEX IV.

Feature	Value	Units
MODEL	RepRap BCN 3D+	
MANUFACTURER	Fundació CIM	
COST	740	€
SPEED	200	mm/s
PRINT LAYER HEIGHT	0,1	mm
PRINT TOLERANCE	0,05	mm
MAX BUILT HEIGHT	200	mm
MAX BUILT WIGHT	210	mm
MAX BUILT LENGTH	240	mm
NOZZLE DIAMETER	0,4	mm
FILAMENT	ABS-PLA-NYLON	

Table 1: RepRap BCN 3D+ printing features [1]

---

<sup>1</sup> RepRap is an open source 3D printing community. <http://reprap.org/wiki/RepRap>

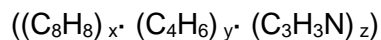
<sup>2</sup> Fundació CIM, Company attached to Barcelona TECH of knowledge engineering and technology management <http://www.fundaciocim.org/es>

## 6 MATERIAL

Reprap 3D+ printer supports ABS, PLA and NYLON as basic and recommended materials. This study has tested all them comparing the resultant mechanical properties and the printing performance in order to know the optimum material for UAV applications.

### 6.1 ABS

ABS (Acrylonitrile butadiene styrene) is a thermo polymer made by styrene and acrylonitrile (strength property) with polybutadiene (rubbery substance). ABS mechanical properties vary with temperature, it can be used between -20°C and 80°C. [2]



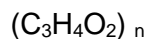
*ABS Chemical formula [2]*

According to the European plastic trade association, the industrial production of 1 Kg of ABS resin in Europe uses an average of 26.48 KW/h [3] and it is derived from natural gas and petroleum.

In the 3D printing technology, ABS is a strong, durable production-grade thermoplastic used across many industries. ABS is an ideal material for conceptual prototyping through design verification and direct digital manufacturing [4]. ABS with FDM technology is able to create real parts direct from digital files, in a variety of standard and custom colors (blue in this study).

### 6.2 PLA

PLA (PolyLactic Acid) is the recommended material for many desktop 3D printers, because it is useful in a broad range of printing applications and has the virtue of being both odorless and low-warp [4].



*PLA Chemical formula [5]*



PLA is also one of the more eco-friendly 3D printing materials available; it is made from annually renewable resources (corn-starch) and requires less energy to process than traditional (petroleum-based) plastics. Outside of 3D printing, PLA is often used in food containers, such as candy wrappers, and biodegradable medical implants, such as sutures [6]. PLA is available in a wide range of colors in both 1.75 mm and 3 mm (white in this study).

### **6.3 NYLON**

Polyamides, better known as nylon (PA), are semi crystalline polymers with magnificent mechanical properties, such as high toughness and brilliant features in regards to sliding and wear resistance [7]. Nylon is a versatile 3D printing material which prints as a bright natural to white with a translucent surface, and can absorb color added post process with most common, acid-based clothing dyes. Unprinted Nylon is extremely sensitive to moisture [8], so taking drying measures during storage and immediately prior to printing is highly recommended for optimal results (translucent in this study).

This study has tested this material using a homemade methodology to reduce NYLON filament humidity level. Before printing, 1000 g NYLON filament coil has been heated during 50 min at 100° C oven temperature and then covered with newspaper pages during 24 hours at room temperature. This process allows user to print 200 mm Z axis parts configured by a PA specific G-code.

### **6.4 Material selection**

A Press method has been used in order to select the optimum material for the 3D printed UAV manufacturing stage. The basic requirements have been:

- Recyclability, because a low cost technology generates many leftover parts.
- Glass transition temperature, because thermal transition phase would collapse UAV structure.

- Material density, since the UAV operational empty weight will be an important feature for the feasibility of the 3D printing technology.
- Tensile modulus, because mechanical properties of the material will be an important feature to support the aerodynamic loads.

Previous materials, ABS, PLA and PA, are the three alternatives since they all meet the main requirements for the selection of the material. Weighting requirements have been estimated equal for all of them except of recyclability, where weighting is the double because the author of this study is environmental friendly.

Materials density has been tested with the available material coils because this information is not included in the Fundació CIM supplied filament. Tested material thread has been 141,5mm length cut and 3mm diameter, using a  $\pm 250 \mu\text{m}$  precision tool.



Figure 2: Available filament ABS-PLA-NYLON Weight test.

	Recyclability	Tg [°C]	Density [g/cm <sup>3</sup> ]	UTS [MPa]
ABS	1,0	105	1,06	44,8
PLA	0,9	65	1,23	57,8
NYLON 6	0,9	58	1,20	70,0

Table 2: Alternatives specifications [6]

These values, Table 2, have been pondered near to 1, see Table 3, according to the best performance in any requirement. The interpretation of the alternatives features has been:

- PLA has been the most interesting alternative in the recyclability value since it is biodegradable. ABS and Nylon are polyamides with the same behavior.
- Glass temperature shows an interesting ABS application for near engine parts. Other material alternatives will require the design of a cooling system.
- Optimum material from density viewpoint has been ABS because its weight is 86% PLA's for the same volume.
- Ultimate tensile strength shows that the most interesting alternative has been Nylon, it has interesting mechanical properties for UAV wing structural performance.

A take decision method, Press in this case, has been used to select the optimum material for 3D printing the UAV, see next tables:

Rating	Recyclability	Tg [°C]	Density [g/cm <sup>3</sup> ]	UTS [MPa]
Factor	2	1	1	1
Relative (Pj)	0,4	0,2	0,2	0,2
Alternatives				
<b>ABS</b>	0,8	1,05	0,94	0,64
<b>PLA</b>	1,0	0,65	0,81	0,83
<b>NYLON 6</b>	0,8	0,58	0,83	1,00

Table 3: Material selection scores table

	Recyclability	Tg [°C]	Density [g/cm <sup>3</sup> ]	UTS [MPa]
<b>ABS</b>	0,320	0,210	0,189	0,128
<b>PLA</b>	0,400	0,130	0,163	0,165
<b>NYLON 6</b>	0,320	0,116	0,167	0,200

Table 4: Material selection appreciation matrix

<b>ABS</b>	0,00	0,11	0,12	0,22
<b>PLA</b>	0,12	0,00	0,09	0,21
<b>NYLON 6</b>	0,07	0,04	0,00	0,11
	0,19	0,14	0,21	

Table 5: Material selection domination matrix

ABS	1,17
PLA	1,46
NYLON 6	0,53

Table 6: Material selection result

The take decision method shows that **PLA** is the most interesting option for the application of this study, UAV, because it is biodegradable while has acceptable mechanical properties, but operational empty weight of the estimated UAV will be 16% greater than the same ABS model and a heat transfer study could be required in the next engine parts.

Since this moment, this study will use white PLA material for all 3D printed parts. The philosophy of this study is to create and develop environment friendly technology because it is not possible to know future applications and repercussion of present researching studies.

### **6.5 PLA tensile test**

PLA material tensile test has been made in the ETSEIAT materials laboratory in May, 9<sup>th</sup> 2014 with the support and help of Dra. Silvia Illescas<sup>3</sup>, an ETSEIAT materials science professor. Standard ASTM D638<sup>4</sup> has been used in this test where the tensile testing machine pulls the sample from both ends and measures the force required to pull the specimen apart and how much the sample stretches before breaking. [9]

Reprap BCN 3D+ is a FDM RMS that uses a 400µm thread of fused PLA. Printing operation is a layer-by-layer process, in the Z axis, that changes PLA properties from isotropic filament to anisotropic when 3D printing part. The reason is that fused thread deposition follows a path, XY plane content, in the machine direction while it is transversal in the perpendicular one and in the Z axis. Thereby UAV design will require tensile test in the two directions, machine direction and transversal direction.

Machine direction (MD) sample is a two layers thickness piece, 800µm that cannot be printed in the XY plane because the bed is at 50°C temperature. Hot bed affects close printed zone by maintaining near  $T_g$  temperature and crystallization percent is different than another zones where cool phase becomes at ambient temperature.

---

<sup>3</sup> Dra. Silvia Illescas. ETSEIAT's professor of materials department [silvia.illescas@upc.edu](mailto:silvia.illescas@upc.edu)

<sup>4</sup> Standards ASTM website: <http://www.astm.org/Standards/D638.htm>

MD sample has been printed in the XZ plane using supporting bridges, see Figure 3, becoming a non-exactly 10 mm along the sample, this design avoid surface different fusion because it is not in contact with hot bed.

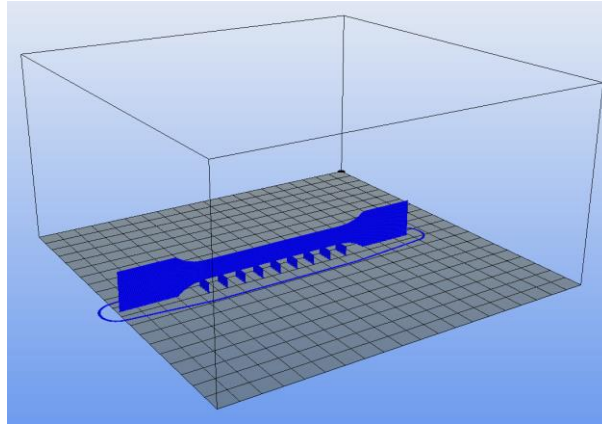


*Figure 3: MD sample G-Code*

After testing the MD sample, see Figure 4, it has been broken in a 1/3 length position, just in a bridge support. This justifies that printing deformation has not affected the sample and results can be estimated as correct.



*Figure 4: PLA 3D printed MD sample*

TD sample has been printed in Z axis because it is the interest of this part test. Figure 5 shows the layer degradation along the height in the printing process. This bad performance of the 3D printing technology is important to be evaluated for 200mm Z axis pieces.

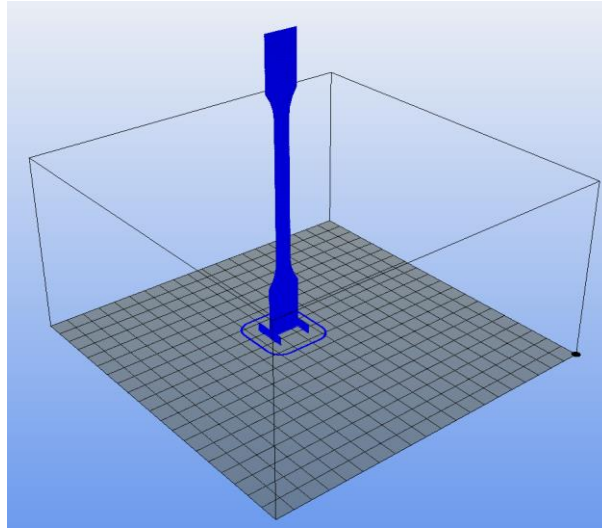


*Figure 5: TD sample G-Code*

In this case the cantilever position of the sample has not been able to support the bed movement inertial, appearing harmonic deformation. After test sample, see Figure 6, it is shown the extreme breakpoint, the middle one has only been an accident during manipulation once the test has been finished. For this reason, this study has estimated that TD test result is lower than in a better sample case, but acceptable since this is the worst situation.



*Figure 6: PLA 3D printed TD sample*

Once MD and TD samples have been tested, this study is able to evaluate the anisotropic behavior of 3D printed parts in function of the two different PLA thread directions when FDM.

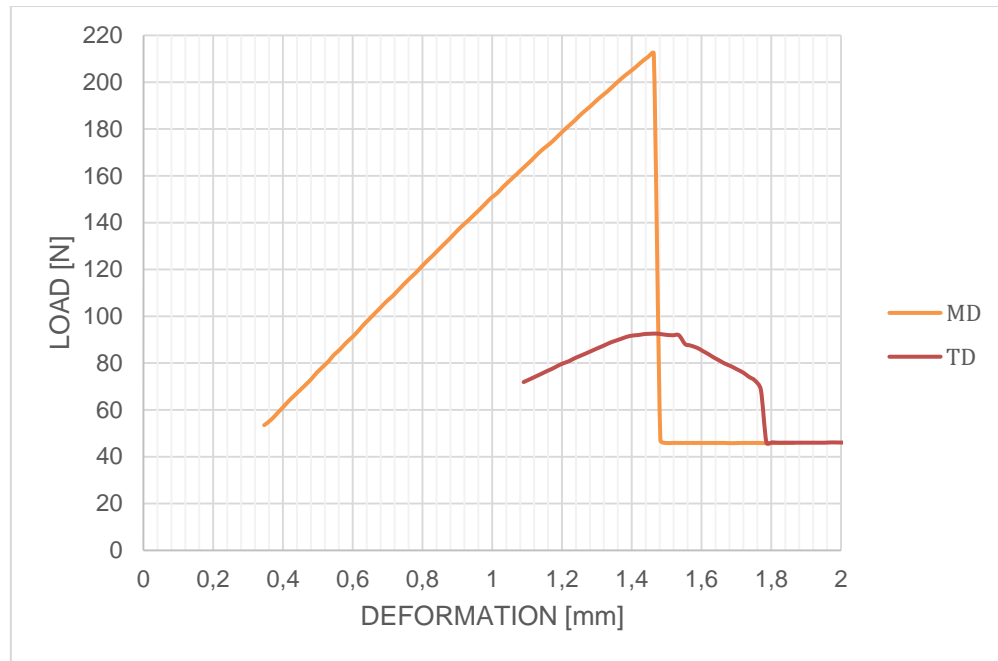


Figure 7: PLA Tensile Test graphic

PLA tensile test result, see Table 7, shows the difference between MD and TD elastic modulus. The test result has been 968MPa for PLA Young Modulus, inside the PLA referenced range (350-2800 MPa) [10]. MD sample is 2.3 times TD, this result is the justification of the tensile test because 3D printing designer must take into account that final part will become anisotropic with a half reduction of mechanical properties in the transversal direction, the Z printing axis.

	width	Thickness	Maximum load	Maximum tensile	Modulus
Units	[mm]	[mm]	[N]	[MPa]	[MPa]
MD	10	0,8	212,297	26,5	968
TD	10	0,8	92,599	11,6	420

Table 7: PLA Tensile Test results

Since PLA material has been selected and the anisotropic behavior of 3D printed parts have been evaluated, this study concludes that the testing stage of the RepRap BCN 3D+ printing technology can start.



## 7 REPRAP 3D PRINTER ANALYSIS

This is an important stage of this study because next UAV application performance will directly depend on the skill and knowledge of new 3D printing technology. The required targets of this stage are:

- STL exportation
- G-Code programming
- Lineal model approximation of the printing configuration performance
- Nonsupport material, complex parts methodology
- Printing time and cost estimation
- Help & support community

### 7.1 STL exportation

STereoLithography is a file format created by 3D Systems<sup>5</sup>. It describes geometry surface of a 3 dimensions object without attributes using a raw unstructured triangulated surface by the unit normal and vertices. STL representation can be ASCII or binary. [11]

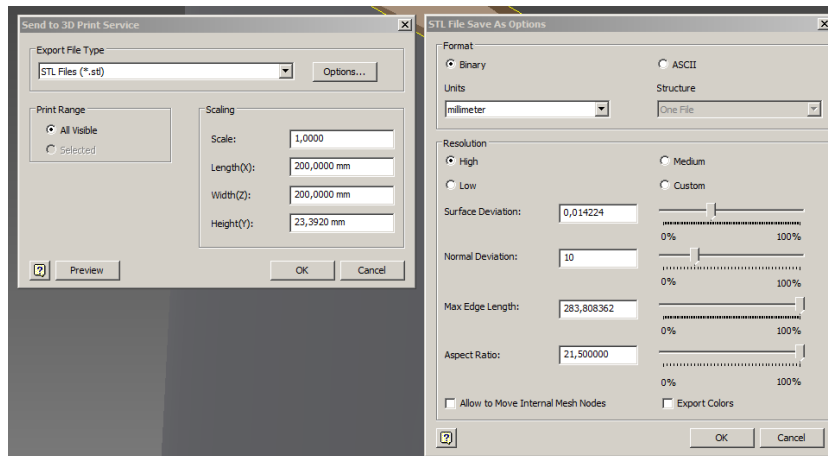


Figure 8: STL exporting command

---

<sup>5</sup> 3D Systems webpage: <http://www.3dsystems.com/>

CAD software has an STL exporting command, see Figure 8. This study has used AutoCAD and Inventor Autodesk<sup>6</sup> software (under student license) where STL command allows users to define accurate exportation.

UAV application requires a specific CAD design. Airfoil design has required a *spline* made by a high number of points and/or a parametric equation of a curved path, therefore the exported STL can become a heavier file. In this study parts with complex surfaces have not been able to be exported because the computer collapses. Due to these computational issues, a logic and trigonometric methodology for complex airfoil design is developed for this study.

Airfoil methodology consists in aligning the Z body axis points from upper and lower chamber line. With this simple concept, more than 4000 pointed polyline airfoils have been exported. The developed method, with high designing performance, permits designing an airfoil with 100  $\mu\text{m}$  accuracy, a similar value to 3D printing precision in the X and Y axis.

This methodology has fixed **100  $\mu\text{m}$  precision** for UAV applications in the 3D printed aerodynamic design. This result is useful in order to define constraints in a computed iteration algorithm.

## **7.2 G-Code programming**

G-Code<sup>7</sup> is used in CNC programming language. It was first developed by MIT Servomechanisms Laboratory in 1950. 3D printing firmware is usable for CNC milling following the NIST<sup>8</sup> RS274NGC G-code standard.[12]

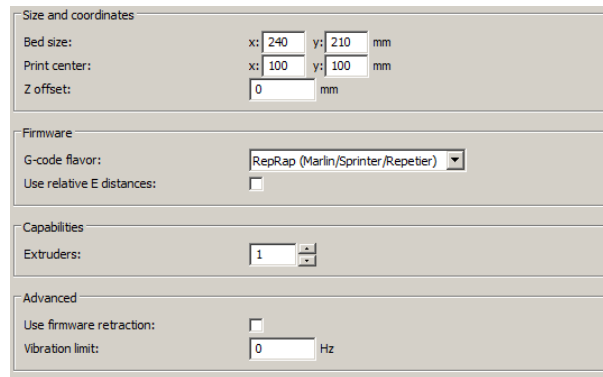
---

<sup>6</sup> Autodesk, Inc. is an American multinational software corporation. <http://www.autodesk.com/>

<sup>7</sup> G-Code is a numerical control (NC) programming language

<sup>8</sup> NIST is the National Institute of Standards and Technology. webpage: [http://www.nist.gov/manuscript-publication-search.cfm?pub\\_id=823374](http://www.nist.gov/manuscript-publication-search.cfm?pub_id=823374)

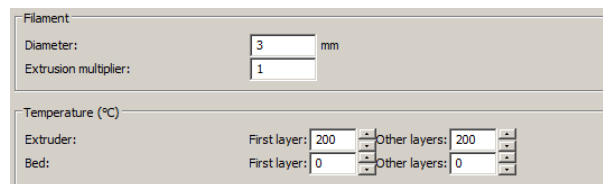
Open source slicer programs, like Slic3r<sup>9</sup>, take a CAD model, slice it into layers, and output the G-Code required for each layer. Printer settings, see Figure 9, have been configured for specific RepRap BCN 3D+.



The screenshot shows the Slic3r printer settings interface. It is divided into four sections: 'Size and coordinates', 'Firmware', 'Capabilities', and 'Advanced'. In the 'Size and coordinates' section, 'Bed size' is set to 240 mm x 210 mm, 'Print center' is 100 mm x 100 mm, and 'Z offset' is 0 mm. The 'Firmware' section shows 'G-code flavor' set to 'RepRap (Marlin/Sprinter/Repeter)' and 'Use relative E distances' is unchecked. The 'Capabilities' section shows 'Extruders' set to 1. The 'Advanced' section shows 'Use firmware retraction' is unchecked and 'Vibration limit' is 0 Hz.

Figure 9: Slic3r printer settings

Filament settings, see Figure 10, allows user to adjust filament diameter and extruder temperature. These configurations depend on the used material and any material has a range of temperature depending on the complexity of the part and the Z axis height.



The screenshot shows the Slic3r filament settings interface. It is divided into two sections: 'Filament' and 'Temperature (°C)'. In the 'Filament' section, 'Diameter' is set to 3 mm and 'Extrusion multiplier' is 1. In the 'Temperature (°C)' section, 'Extruder' has 'First layer' at 200 °C and 'Other layers' at 200 °C, and 'Bed' has 'First layer' at 0 °C and 'Other layers' at 0 °C.

Figure 10: Slic3r filament settings

Layers and perimeters settings, see Figure 11, is the key optimization adjustment. Layer height is only the distance between two Z axis layers, but it affects to:

- The minimum angle printable for non-supported parts
- The wall thickness because the same material is deposited into a different height layer.

---

<sup>9</sup> Slic3r is an OPEN SOURCE that converts STL files into G-CODE printing instructions. <http://slic3r.org/>

The screenshot shows the 'Layers and Perimeters' settings in Slic3r. It is divided into several sections:
 

- Layer height:** 'Layer height' is set to 0.4 mm, and 'First layer height' is set to 0.35 mm or %.
- Vertical shells:** 'Perimeters (minimum)' is set to 3, and 'Spiral vase' is unchecked.
- Horizontal shells:** 'Solid layers' are set to 3 for both 'Top' and 'Bottom'.
- Quality (slower slicing):** 'Extra perimeters if needed' is checked. 'Avoid crossing perimeters' is unchecked. 'Start perimeters at:' has 'Concave points' and 'Non-overhang points' both unchecked. 'Detect thin walls' is checked. 'Detect bridging perimeters' is checked.
- Advanced:** 'Randomize starting points' and 'External perimeters first' are both unchecked.

Figure 11: Slic3r layers and perimeters

Infill is the internal structure between perimeters. Figure 12 shows the Infill menu where the user can adjust density, pattern and angle. This is a dangerous adjustment because, while CAD is a 100% user design controller, Infill is programmed and can only be adjusted by an iteration process.

The screenshot shows the 'Infill' settings in Slic3r. It is divided into several sections:
 

- Infill:** 'Fill density' is set to 0.4. 'Fill pattern' is set to 'honeycomb'. 'Top/bottom fill pattern' is set to 'rectilinear'.
- Reducing printing time:** 'Combine infill every:' is set to 1 layers. 'Only infill where needed' is unchecked.
- Advanced:** 'Solid infill every:' is set to 0 layers. 'Fill angle' is set to 45 degrees. 'Solid infill threshold area' is set to 70 mm². 'Only retract when crossing perimeters' is checked. 'Infill before perimeters' is unchecked.

Figure 12: Slic3r infill

Fill patterns and density have been tested and showed in a matrix, see Figure 13. Columns are the pattern type and rows are the Infill density. Test pattern types have been:

- Honeycomb
- Concentric
- Line
- Rectilinear
- Hilbert curve

- Archimedean Chords
- Octagram Spiral

The variation of density parameters in the rows from left to right has been:

Density = 20 x #column [%], resulting a 20%, 40%, 60% and 80%.

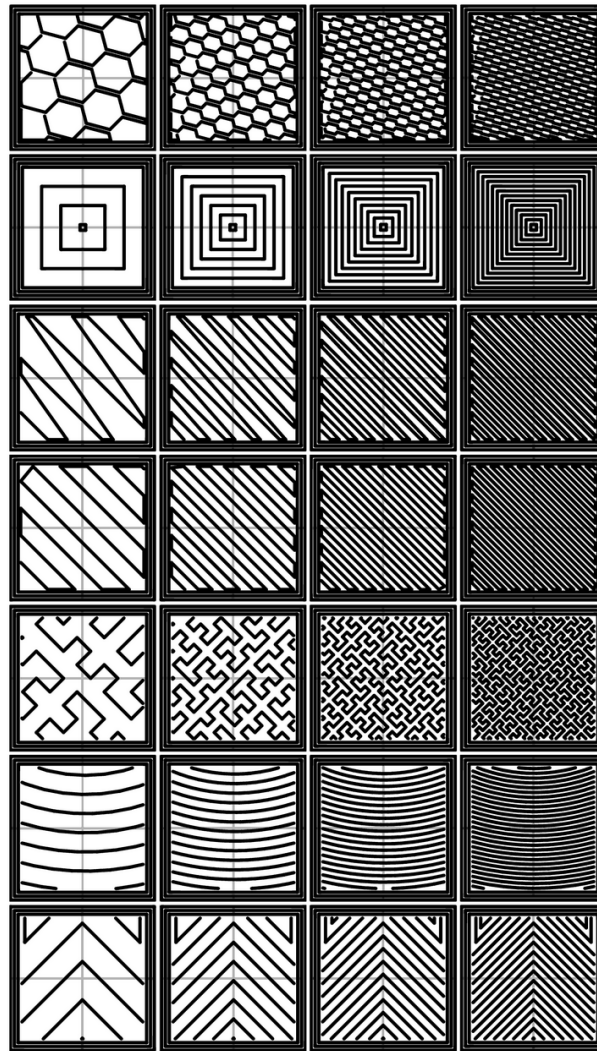


*Figure 13: Slic3r Infill patterns and density matrix [13]*

The structural design for UAV applications can be high accuracy optimized by using a Finite Element Method (FEM). In this case the G-Code generation of the 3D printed parts has to maintain FEM design and accuracy. Therefore the use of a rapid slicer requires a skilled user and a G-Code simulation analysis.

Another option for G-Code generation is to use a lower level library. In this way, Mecode is an interesting open source library written in python and licensed under the MIT license. This study has not developed this software since slicer has become the optimum option.

In order to understand the importance of this 3D printing stage in the UAV applications and its complexity, slicing stage for 3D printing a wing part of 200mm chord and 185mm length requires the programming of near 200.000 G-code lines. This complex stage becomes more simple and rapid by using slicer software that provides the automatic G-code generation, although less accuracy.

### **7.3 Linear model approximation**

Linear model approximation is a statistic method to estimate the functional relationship between a process result and those control factors [14]. In this study, this means an equation to adjust 3D printer configuration in function of the specific requirements. Linear model tool will allow the users to analyze tested parts and be able to define an analytic algorithm to preview printed features.

3D printing *control factors* have been the Z axis height and speed. The reason is that 400  $\mu\text{m}$  fused PLA thread is a constant volume and it is deposited in a differential volume that depends on the Z axis weight and on the speed of the extruder. As Z axis height and speed are increased, perimeter thickness is reduced. Thereby control factors have been:

- $X_1$ : Z axis height [mm]
- $X_2$ : Speed [mm/s]

Z axis height has been tested in 3 levels: 0.1 mm, 0.2 mm and 0.25 mm. The first one is the minimum level for the RepRapBCN 3D+ and the last one is an estimated maximum value for standard performance since it is 62.5 % of the thread diameter.

Speed has been tested in 3 levels: 60 mm/s, 80 mm/s and 90 mm/s. The last one is the maximum 3D printer value and the first one is recommended for high quality performance.

The linear model *answer* is the final performance that we want to estimate. In the UAV application the interesting features are weight and mechanical properties. The state of the art analysis done in ANNEX I attachment, has showed that operational empty weight must be improved in order to make this technology feasible. Therefore the chosen property is weight.

- Y: weight [g]

Factor number of levels;	$k_1 = k_2 = 3$	
Each combination have two replicas;	$r = 2$	
Total number of experiences;	$n = 18$	
Number of different experimental combinations;	$q = 9$	
Model number of terms;	$p \leq q$	
Maximum degree of the factor;	$X_1 \leq k_1 - 1$	$X_1^2$
	$X_2 \leq k_2 - 1$	$X_2^2$

The first proposed model has the maximum terms and coefficients has been estimated with the 3d printed samples:

$$\hat{Y} = \hat{\beta}_0 + \hat{\beta}_1 X_1 + \hat{\beta}_2 X_2 + \hat{\beta}_{12} X_1 X_2 + \hat{\beta}_{11} X_1^2 + \hat{\beta}_{22} X_2^2 \quad (1)$$

$X_1 \setminus X_2$	60		80		90	
0.25	0,20	0,20	0,19	0,20	0,19	0,19
0.2	0,20	0,21	0,20	0,20	0,19	0,20
0.1	0,21	0,21	0,20	0,21	0,20	0,20

Table 8: Weight measurements of the linear model experimentation.

Figure 14 shows the matrix of the 3D printed samples from the same STL. Like in the previous table, rows are  $X_1$  factor and columns  $X_2$  factor.

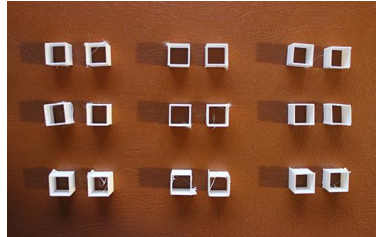


*Figure 14: Samples matrix*

The perfect and excellent yield figure would be the same weight for every sample, since it is the same part for any sample. This test demonstrates that the weight of the final part depends on the parameters.

The surface analysis is an interesting tool to answer weight variability. Comparing the (0.25, 60) and (0.10, 90) sample surfaces, see Figure 15, we can see that the 0.25mm height has been marked on the surface while reducing this value is 3D printed as an smoothed surface. Speed parameter has not been showed into the surface roughness.

Another interesting measurement of all the samples is the perimeter thickness. Using a Ratio scale within  $\pm 10\mu\text{m}$  precision in this measurement. A Student statistic, since unknown variance, has evaluated with 95 percent of reliability a  $600\mu\text{m}$  wall thickness.

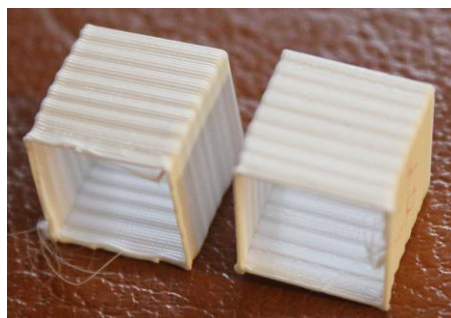


*Figure 15: (0.25, 60) and (0.10, 90) sample surfaces*



Next step has been the matrix of the model computation:

$$Y = \begin{pmatrix} 0,20 \\ 0,20 \\ 0,19 \\ 0,20 \\ 0,19 \\ 0,19 \\ 0,20 \\ 0,21 \\ 0,20 \\ 0,20 \\ 0,19 \\ 0,20 \\ 0,21 \\ 0,21 \\ 0,20 \\ 0,21 \\ 0,20 \\ 0,21 \\ 0,20 \end{pmatrix} \quad X = \begin{pmatrix} 1 & 0.25 & 60 & 15 & 0.0625 & 3600 \\ 1 & 0.25 & 60 & 15 & 0.0625 & 3600 \\ 1 & 0.25 & 80 & 20 & 0.0625 & 6400 \\ 1 & 0.25 & 80 & 20 & 0.0625 & 6400 \\ 1 & 0.25 & 90 & 22.5 & 0.0625 & 8100 \\ 1 & 0.25 & 90 & 22.5 & 0.0625 & 8100 \\ 1 & 0.2 & 60 & 12 & 0.04 & 3600 \\ 1 & 0.2 & 60 & 12 & 0.04 & 3600 \\ 1 & 0.2 & 80 & 16 & 0.04 & 6400 \\ 1 & 0.2 & 80 & 16 & 0.04 & 6400 \\ 1 & 0.2 & 90 & 18 & 0.04 & 8100 \\ 1 & 0.2 & 90 & 18 & 0.04 & 8100 \\ 1 & 0.1 & 60 & 6 & 0.01 & 3600 \\ 1 & 0.1 & 60 & 6 & 0.01 & 3600 \\ 1 & 0.1 & 80 & 8 & 0.01 & 6400 \\ 1 & 0.1 & 80 & 8 & 0.01 & 6400 \\ 1 & 0.1 & 90 & 9 & 0.01 & 8100 \\ 1 & 0.1 & 90 & 9 & 0.01 & 8100 \end{pmatrix} \quad \hat{\beta} = \begin{pmatrix} \hat{\beta}_0 \\ \hat{\beta}_1 \\ \hat{\beta}_2 \\ \hat{\beta}_{12} \\ \hat{\beta}_{11} \\ \hat{\beta}_{22} \end{pmatrix} \quad e = \begin{pmatrix} e_1 \\ e_2 \\ e_3 \\ e_4 \\ e_5 \\ e_6 \\ e_7 \\ e_8 \\ e_9 \\ e_{10} \\ e_{11} \\ e_{12} \\ e_{13} \\ e_{14} \\ e_{15} \\ e_{16} \\ e_{17} \\ e_{18} \end{pmatrix}$$

$$Y = X \hat{\beta} + e \quad (II)$$

Least squares estimation method has been used in order to get minimum e values.

$$\hat{\beta} = (X' X)^{-1} X' Y \quad (III)$$

Open source computational software have been used to solve this matrix equation:

$$(X' X)^{-1}$$

$$\begin{pmatrix} 213.45796 & -191.74036 & -5.42276 & 1.29082 & 262.96296 & 0.03472 \\ -191.74036 & 1773.12925 & 1.29082 & -7.04082 & -3555.55556 & 0.00000 \\ -5.42276 & 1.29082 & 0.14651 & -0.01684 & 0.00000 & -0.00096 \\ 1.29082 & -7.04082 & -0.01684 & 0.09184 & 0.00000 & 0.00000 \\ 262.96296 & -3555.55556 & 0.00000 & 0.00000 & 10370.37037 & 0.00000 \\ 0.03472 & 0.00000 & -0.00096 & 0.00000 & 0.00000 & 0.00001 \end{pmatrix}$$

$$X' Y$$

$$\begin{pmatrix} 3.600000 \\ 0.655500 \\ 275.100000 \\ 50.090000 \\ 0.133425 \\ 21585.000000 \end{pmatrix}$$

$\hat{\beta}$ 

```
0.183333333338983
0.050000000006171
0.000916666669485
0.000000000003557
-0.333333333339636
-0.000008333343710
```

Finally the first computed linear model approximated equation has been:

$$\hat{Y} = 0.1833 + 0.05 X_1 + 0.0009 X_2 + 3.557E - 12 X_1 X_2 - 0.3333 X_1^2 - 0.000008 X_2^2 \quad (IV)$$

Significance of first model has been studied, using ANOVA<sup>10</sup> statistic tool, to evaluate computed coefficients. Table 9 shows the estimated values and error for each sample using the first linear model. Table 10 shows least squares method and type errors of the estimated coefficients.

#	X1	X2	Y	Ŷ estimated	e
1	0.25	60	0.20	0.200	0.000
2	0.25	60	0.20	0.200	0.000
3	0.25	80	0.19	0.195	-0.005
4	0.25	80	0.20	0.195	0.005
5	0.25	90	0.19	0.190	0.000
6	0.25	90	0.19	0.190	0.000
7	0.20	60	0.20	0.205	-0.005
8	0.20	60	0.21	0.205	0.005
9	0.20	80	0.20	0.200	0.000
10	0.20	80	0.20	0.200	0.000
11	0.20	90	0.19	0.195	-0.005
12	0.20	90	0.20	0.195	0.005
13	0.10	60	0.21	0.210	0.000
14	0.10	60	0.21	0.210	0.000
15	0.10	80	0.20	0.205	-0.005
16	0.10	80	0.21	0.205	0.005
17	0.10	90	0.20	0.200	0.000
18	0.10	90	0.20	0.200	0.000

Table 9: Linear model estimated error

---

<sup>10</sup> ANOVA, **Analysis of variance** is a collection of statistical models used to analyze the differences between group means and their associated procedures.

---

$\bar{Y}$	0.20
SQR	0.000200000000076579
SQEx	0.000599999999993358
SQT	0.000800000000069937
R <sup>2</sup>	0.75
QMR	1.66667E-05
QMEx	0.00012
S $\beta_1$	0.17190740
S $\beta_2$	0.001562637
S $\beta_{12}$	0.001237201
S $\beta_{11}$	0.41573971
S $\beta_{22}$	1.29099E-05

Table 10:  $\beta_j$  Type errors

	v	SQ	QM	Fcomp (Snedecor)	F $\alpha$ (5,12,0.05)
Regression	5	0.000599999999993358	0.00012	7.2	3.11
Rest	12	0.000200000000076579000	1.66667E-05		
Total	17	0.000800000000069937			

Table 11: First linear model ANOVA

ANOVA regression, see Table 11, shows that the estimated linear model is significantly with 5% risk, since  $F_{\text{computed}} > F_{\alpha}$ . Thereby we can evaluate coefficients significance.

	Coefficients	Type error	T (student)	T (12, 0.025)	Eliminate
$X_1$	0.05	0.1719074	-0.1219074	$\pm 2.179$	
$X_2$	0.000916667	0.001562637	-0.00064597	$\pm 2.179$	
$X_1 X_2$	3.557E-12	0.001237201	-0.001237201	$\pm 2.179$	
$X_1^2$	-0.333333333	0.41573971	-0.749073043	$\pm 2.179$	
$X_2^2$	-8.33334E-06	1.29099E-05	-2.12433E-05	$\pm 2.179$	X

Table 12: First linear model coefficients significance

T student is a bilateral statistic; therefore most near to zero Student coefficient is the less significant value. The first linear model  $X_2^2$  coefficient has been eliminated.

Coefficient elimination requires restarting the process from the second linear model, without the eliminated term:

$$\hat{Y} = \hat{\beta}_0 + \hat{\beta}_1 X_1 + \hat{\beta}_2 X_2 + \hat{\beta}_{12} X_1 X_2 + \hat{\beta}_{11} X_1^2 \quad (V)$$

Computed coefficients have been:

$$\hat{Y} = 0.2279 + 0.0493 X_1 - 0.0003 X_2 - 0.00006 X_1 X_2 - 0.3316 X_1^2 \quad (VI)$$

	v	SQ	QM	Fcomp (Snedecor)	F $\alpha$ (4,13,0.05)
Regression	4	0.000587517769515855	0.000146879	8.855853	3.18
Rest	13	0.000215612524390950000	1.65856E-05		
Total	17	0.000803130293906805			

Table 13: Second linear model ANOVA

	Coefficients	Type error	T (student)	T (13, 0.025)	Eliminate
$X_1$	0.049336	0.171184341	-0.121848341	$\pm 2.16$	
$X_2$	-0.000303	0.000238999	-0.000541999	$\pm 2.16$	X
$X_1 X_2$	-0.000061	0.001234168	-0.001295168	$\pm 2.16$	
$X_1^2$	-0.331614	0.413656078	-0.745270078	$\pm 2.16$	

Table 14: Second linear model coefficients significance

Second iteration less importance term has been:  $X_2$ . This elimination is double because  $X_1 X_2$  depends on it. Therefore, using previous computation method, third linear model has been:

$$\hat{Y} = \hat{\beta}_0 + \hat{\beta}_1 X_1 + \hat{\beta}_{11} X_1^2 \quad (VII)$$

New computed coefficients have been:

$$\hat{Y} = 0.203375 + 0.049409 X_1 - 0.33161 X_1^2 \quad (VIII)$$

	v	SQ	QM	Fcomp (Snedecor)	F $\alpha$ (2,15,0.05)
Regression	2	0.000299999714786299	0.00015	+4.499992	+3.68
Rest	15	0.000500000372994949000	3.33334E-05		
Total	17	0.000800000087781249			

Table 15: Third linear model ANOVA

	Coefficients	Type error	T (student)	T (15, 0.025)	Eliminate
X <sub>1</sub>	0.049409	0.202241264	-0.152832264	±2.131	X
X <sub>1</sub> <sup>2</sup>	-0.331614	0.586426556	-0.918040556	±2.131	

Table 16: Third linear model coefficients significance

At the last iteration, linear model only has de quadratic Z height parameter.

$$\hat{Y} = \hat{\beta}_0 + \hat{\beta}_{11} X_1^2 \quad (IX)$$

Last computed coefficients have been:

$$\hat{Y} = 0.207093 - 0.18918 X_1^2 \quad (X)$$

	v	SQ	QM	Fcomp (Snedecor)	F $\alpha$ (1,16,0.05)
Regression	1	0.000297972971930700	0.000297973	+9.496635	+4.49
Rest	16	0.000502027052920550000	3.13767E-05		
Total	17	0.000800000024851249			

Table 17: Third linear model ANOVA

ANOVA regression, see Table 17, shows that the estimated linear model is significantly with less than 5% risk, see that  $F_{\text{computed}} > F_{\alpha}$ .

Once the model is admissible, this study has evaluated de Normal and constant variance hypothesis. Figure 16 shows the non-axis residual graph to see the randomly component of rest (e), justifying non-pattern existence. Probabilistic graph has been computed to check previous hypothesis resulting an admissible model.

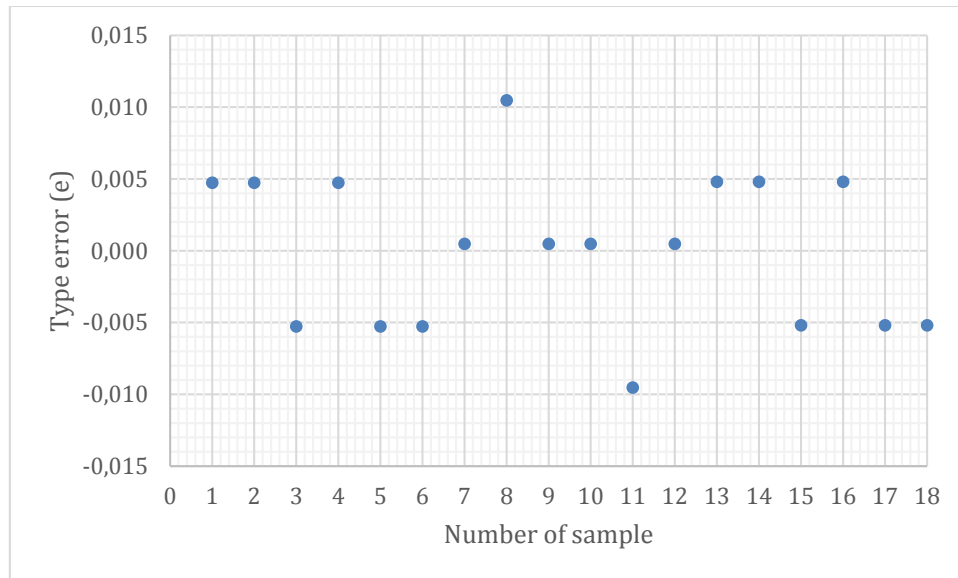


Figure 16: Rests (e) versus average Y.

This linear model can only be applied in the tested range and it shows that Z height is a more significant parameter than printing speed parameter.

The interesting application of previous linear model in this study is that UAV wing has a large surface with accurate airfoil shape, but do not support lift torque while total weight increases. For this reason a thin perimeter is an excellent performance for 3D printing technology in UAV applications. This linear model allows user to optimize weight performance using the maximum Z axis height while smooth requirements.

#### 7.4 Nonsupport material

3D printing is under gravity field, therefore cantilevers and bridges require support material. Since support material is not a final part, an environmental friendly decision

has been taken in order to eliminate it and develop this technology without useless material.

High performance with no supporting material requires a specific CAD design methodology. According to this, three strategies for 3D printing designers are developed in this study:

- TREE
- CHEDDAR
- CLICK
- STOP PRINTING

The definition and justification of these key strategies has been developed in the testing stage.

### ***7.5 Printing time and cost estimation***

Printing time can be estimated from the slicer software, but it is not an interesting feature to be optimized since this is a rapid manufacturing system with a high performance in printing time. Printing speed range is from 60 mm/s to 90 mm/s and linear model has demonstrated that a high printing speed affects the weight of the part by reducing weight while increasing speed. Therefore the maximum speed is the optimum adjustment of this parameter for lightweight parts.

Cost estimation is also checked in this study. Fundació CIM has an accurate information about Reprap 3D printer energy cost since they have a 3D printing service for the UPC community with a 0.12 €/cm<sup>3</sup> cost. The estimated cost for home printing, providing that the costumer already has the 3D printer, has been 0.05€/cm<sup>3</sup> (material and power). [15]

### ***7.6 Help & support community***

3D printing technology requires a continued updating, configuration and calibration. R&D Fundació CIM department [16] has helped this study in the device assembly and performance for UAV applications.

Reprap BCN website forum is a key support reference for 3D printer beginners. New materials have been beta tested, like ASB premium, new printing configurations have been adjusted for own application requirements and updating configurations have been minutely defined.



## 8 PRINTING TEST

Testing stage is a 3D printing process with the most interesting models to know 3D printing technology performance. The most tested model has been a Red Eyed Tree Frog, see because it is a small part with a perfect shape in order to evaluate infill, quality and available printing angles in the critical direction, see Figure 17.

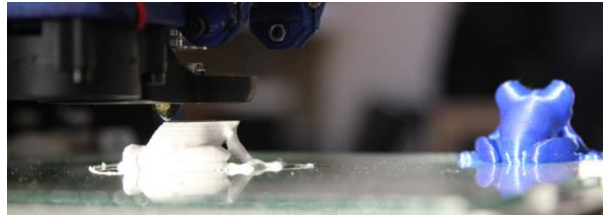


*Figure 17: Red Eyed Tree Frog printing test*

Another model has been used for mechanical properties, the standard beam shapes. During this process this study has been focused in the next factors:

- Starting print calibration and Bed fixation
- Fluid mechanic analysis
- TREE
- CHEDDAR
- CLICK
- STOP PRINTING
- Lattice 3D honeycomb
- Airfoil
- Maximum Z axis printing

This document will not explain basic features of 3D printing process since it is recommended by the own experience and there is a specific methodology for any device. Therefore this part has been focused in the 3D printing process for UAV applications.

### **8.1 Start printing calibration and bed fixation**

The calibration of the bed is an easy stage that has to be checked in any printing process. The main requirement for the start 3D printing stage has been the use of lacquer for the part fixation to the hot bed.

### **8.2 Fluid mechanics analysis**

Previous linear model, 0, has been used in the frog model in order to evaluate the accuracy and for being able to estimate its features. The result has been an excellent weight performance that allows optimizing weight in function of the G-Code configuration.

The 3D printing test of multiple frog models with infill structure has become a surprising stage of this study because the linear model information has allowed to print the same model with different final weight, only with the configuration of different parameters, the speed and the Z axis height. The final weight of the Frog, 3D printed model, has been measured between 5,47g to 6,88g in function of previous parameters, becoming a weight estimation of  $6.175g \pm 11.42\%$ . Since the aim of this study is the feasibility of 3D printing for UAV applications, the final weight optimization depends on the slicer configuration; thereby auto-slicing 3D printers are not feasible for lightweight applications.

RepRap BCN 3D+ material is a fused PLA thread of 400  $\mu\text{m}$  diameter, see Figure 18, which emerges from the 220°C heated extruder. **CAUTION: never touch it without hand protection.**

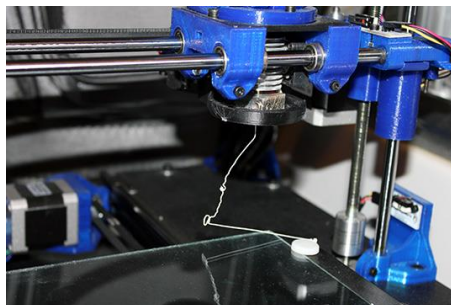


Figure 18: PLA 400  $\mu\text{m}$  thread

Going farther with 3D printing weight performance 2 STL of the same frog has been sliced, where the only difference has been the *printing speed* or *layer height*, and the G-code files have shown that CNC instructions have been exactly the same for the X, Y and E values, where E is the extruder engine instruction. Demonstrating that the “perimeter\_speed” and “layer\_height value” are configured in the printer firmware.

RepRap 3D printer has a stepped motor for the extruder movement, becoming a configuration parameter unit: “x” steps to move 1 mm. Arduino firmware configures the caudal in function of the previous value using next parameters:

```
StepsPerTurn = 200 // Most stepper motors have 1.8 Degree per step (some 0.9)
BeltDistance = 5mm // Distance between repeating grooves. T5 belt => 5mm
GroovesInPulley = 8 // 8-10 are common values
Substepping = 16 // 16 Sub steps for a full step needed
StepsPerMM = StepsPerTurn*Substepping/ (BeltDistance*Substepping) = 200*16/ (5*8) = 80
```

This study has not deepened in firmware programming because the previous linear model is a good estimation to simulate this performance.

According to the previous justification, one hypothesis of this study has been the constant PLA flow in function of the “perimeter\_speed” and “layer\_height” parameters. With this hypothesis this study is able to starts the fluid mechanics evaluation.

Integral continuity equation [17]:

$$\frac{\partial}{\partial t} \int_{VC} \rho dV + \int_{SC} \rho \vec{v} d\vec{s} = 0 \quad (XI)$$

Control volume has been defined as the extruder and the differential volume of PLA thread, without material leakage. Therefore, continuity equation implies that all the fused PLA is deposited in the 3D printed part.

Volumetric flow:

$$Q = \int_S V_n dA \quad (XII)$$

Where  $dA = \pi r^2 = 0.126\text{mm}^2$ , is the area of the 0.4mm diameter calibrated extruder and  $V_n$  is a function of configured parameters.

Mass flow:

$$\dot{m} = Q\rho = \rho \int_S V_n dA \quad (XIII)$$

Where  $\rho$  is the PLA density=1.23 g/cm<sup>3</sup>, measured in previous stage.

In order to estimate  $V_n$  this study has evaluated the 0.6mm thickness, while G-Code parameters have been fixed in (0.25, 90) factors, because this is the best weight performance for the UAV application.

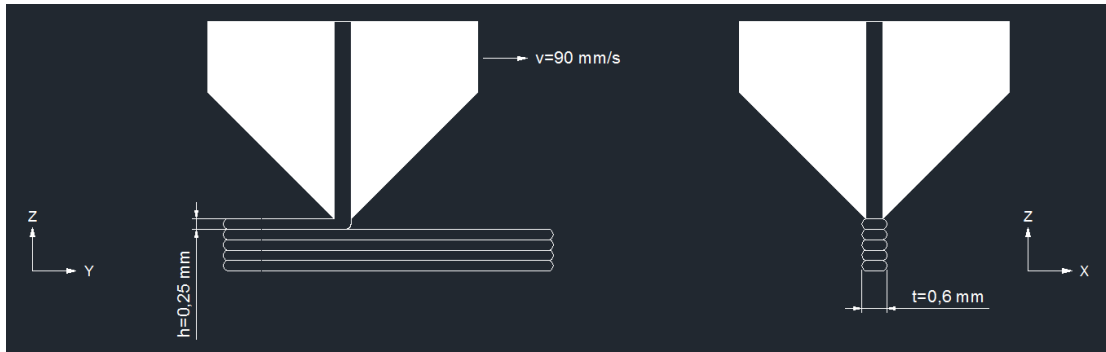


Figure 19: 3D printing process sketch

Figure 19 shows the 3D printing process while the extruder deposits the fused PLA. According to 0.6mm wall thickness, 0.4mm PLA thread diameter and 0.25 mm layer height: deposited PLA has been 0.1373 mm<sup>2</sup> area and 1.4916 mm perimeter and the volume of a 90mm length layer has been 12.357mm<sup>3</sup>.

According to previous hypothesis and computation:

$$Q = 12.357 \frac{mm^3}{s} = 0.126mm^2 V_n \quad (XIV)$$

$$V_n = 98 \frac{mm}{s} \quad (XV)$$

$$\dot{m} = 0.0152 \frac{g}{s} \quad (XVI)$$

It has been demonstrated the optimum configuration of the **printing speed** and the **layer height** for lightweight applications. Thereby from this moment: **(0.25, 90)** factors will be used in this study. Since 3D printing slicer has been configured with the best performance in lightweight materials, this study has been able to develop the 3D printing methodology.

### 8.3 TREE method

The first method developed for this study has been called TREE because it is a tree shape design. UAV complex parts like the winglet requires the knowledge of the maximum differential angle available from the printer Z axis, or the complementary one. Frog model has a near to 60° angle between belly path and Z axis.

Due to the 60° angle, this study has designed a testing part with different angle measurements in a (70-85) range within 5° differential steps. Figure 20 shows 4 designed cantilevers with Z axis angle of 85-80-75-70. In order to be printed correctly, a basement has been added because hot bed could deform starting basement.



Figure 20: Angle tester model

At the end of the printing test, see Figure 21, this study has been able to evaluate the maximum TREE angle in 70°. This value is justified since this angle cantilever is the only one supported.

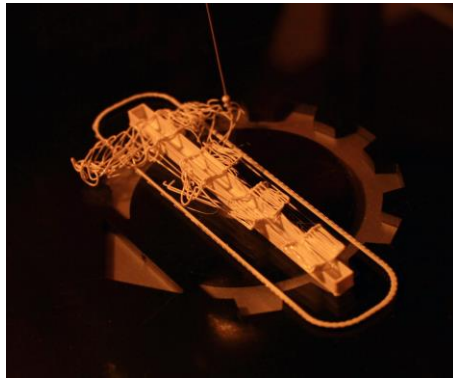


*Figure 21: Maximum TREE angle test*

Trigonometry cannot explain this growing performance because the available maximum angle would be  $25^\circ$ . And the author of this project does not have the knowledge and tools to evaluate fluid dynamics performance because the actual  $20^\circ$  value depends on the next random factors:

- Airflow velocity, the PLA thread is affected for the environment.
- Room temperature, when material is flowing and starts cooling, since the room temperature is lower than extruder temperature, the fused thread is randomly oriented in function of the retracted vector.
- XYZ printer precision, because the extruder has a manufacturer estimation of  $\pm 50\mu\text{m}$  precision and this factor affects maximum angle.
- Extruder pressure, stepped extruder activation do not have a constant PLA pressure and the flow velocity depends on it.

All this factors have not been evaluate for this study and only have been able to estimate a randomly “S” path, see Figure 22, that have allowed the correct layered deposition in some differential parts becoming an actual performance.

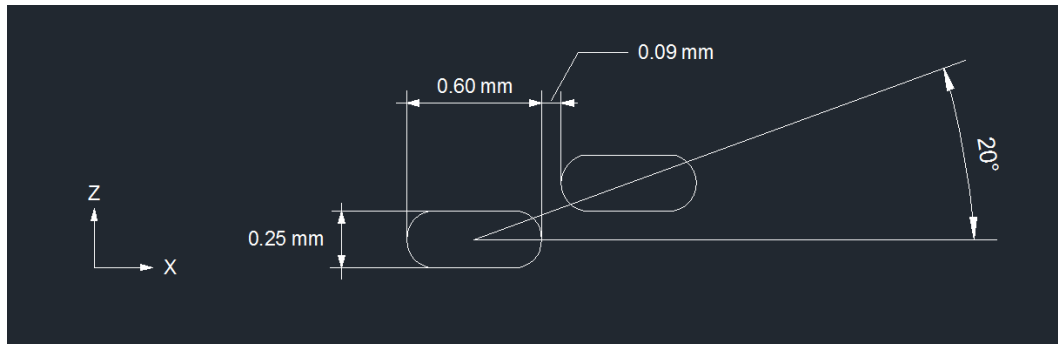


Figure 22: TREE maximum degree collapse

Once the maximum angle has been 70° evaluated, and applying a 5% safety factor reduction, the **maximum TREE angle is 66°**, used in the CHEDDAR methodology, /see next section).

#### 8.4 CHEDDAR method

This method has been called CHEDDAR because it allows the inside part support starting from perimeters by creating bridges. The interest of this skilled design is weight optimization for vessel shapes, when high Z axis zone requires inside printing or horizontal surfaces in the top side.

Standard 3D printing technologies use supporting material by printing all the core and diluting if after printing or an infill structure only required to support the top cap. Therefore, the only requirement of this extra cost is to support, the aim of this method.

This method has been explained by an airfoil example. For a 200mm Z axis airfoil with 200mm chord, the part has been 603cm<sup>3</sup> volume. If the same part is naked, with only 80µm perimeter, it is 35.04 cm<sup>3</sup> volume.

In the CHEDDAR methodology, see Figure 23, the extra volume required for the infill bridge and the top cap has been computed using trigonometric relationship.

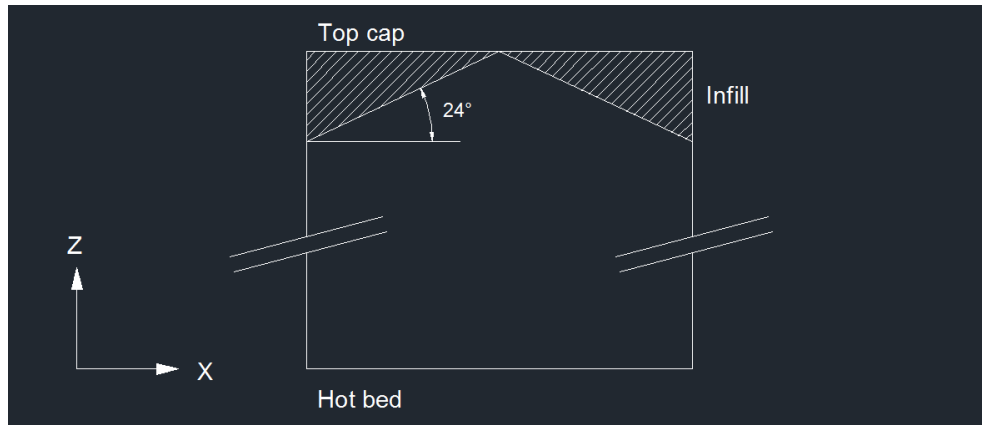


Figure 23: CHEDDAR CAD design

$$V_T = S_T \frac{x \tan 24^\circ}{4} \quad (XVII)$$

Where  $V_T$  is the added volume,  $S_T$  is the top cap surface and  $x$  is the top average thickness. Z axis dimension has been evaluated with the TREE 66° angle, where 24° is the complementary angle.

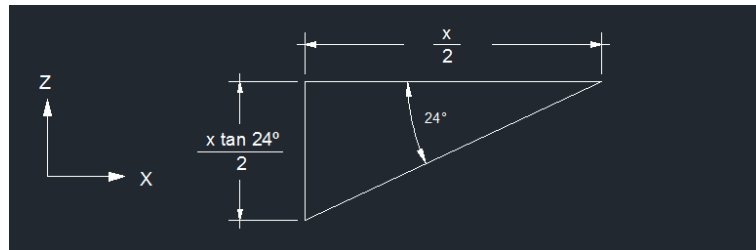


Figure 24: CHEDDAR trigonometric relationship

The volume required to print top cap has been computed in 5.34 cm<sup>3</sup>. Therefore the total volume part is 40.38 cm<sup>3</sup>, 6.7% of the material used with support material.

Comparing with a typical infill for core part, the material wasted with the CHEDDAR method is only 16.6% of the 40% Infill support, demonstrating the interest of the development of this method in order to reduce part cost and printing time.



## 8.5 *CLICK method*

For mobile parts CHEDDAR method cannot be used since it is not possible to break the bridge, thereby CLICK system has been developed.

CLICK methodology has been specially designed for mobile parts like rudder, elevator or aileron in the UAV application. It is called click because once the printed part is finished the designer have to break the weak junction. The study of this method requires a G-Code simulator, in this case the Repetier Host open source software.

The tested part for this application has been the elevator, see Figure 25, where the fixed part has the connecting element inside the mobile part. Since the traditional manufacturing systems cannot build the complete part, fixed and mobile, in the same stage. CLICK method's aim is to print the two parts together and avoid extra material between connections.

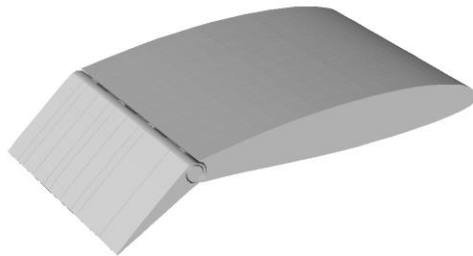


*Figure 25: Aileron CLICK method testing model*

G-Code generated, see Figure 26, can be simulated by layers. The CLICK methodology consists in taking advantage of the 3D printing previous knowledge. The key is to create a small deformation between mobile parts that fixes them. Explanation:

1. Transition layers. In this zone the parts have been printed only perimeters, there is not support material or bridges.
2. Mobile part bottom opening. This layer shows the opened perforation that controls deflection angle, which can be different in both directions.
3. CLICK key. In this layer starts the connection between the two pieces. The fixed one is inserted into the mobile one. The non-supported circle generated

inside the mobile part has small deformation getting in contact with the mobile part, allowing the deposition.

4. Connection layer. Since the previous layer has been supported this one do not have deformation and the only specification is the separation between circles.
5. Mobile part top opening. Like in the layer 2, connection ends while maintaining the perforation. Inside, cylinder printing continues to ensure the clamp length.
6. Finishing layer. This is the last layer where inside cylinder still grows. Since this layer the process is restarted to first according to the connecting separation designed.

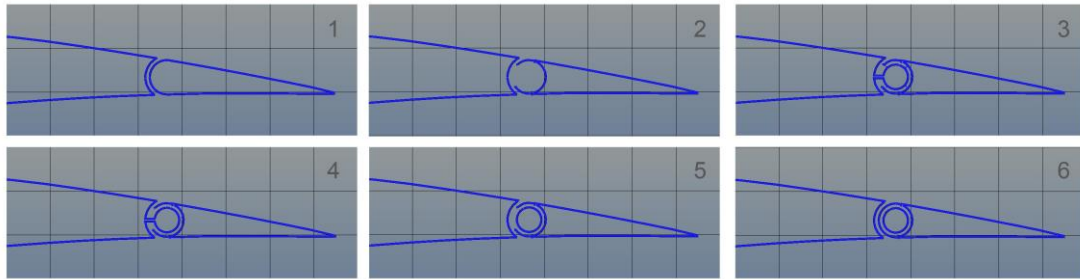


Figure 26: Elevator G-Code layers simulation

The CLICK deformation of this process requires skilled designer and experience. The added thread, that will fix two parts while printing, could be one part deformation or shared. Previous TREE methodology has demonstrated a randomly performance which affects CLICK accuracy. In case of a bad CLICK, where the circle is not supported by the close fixed part, printing pause could be an interesting help to solve it and restart printing.

## 8.6 STOP PRINTING method

This method consists in pause the printing process in order to modify some thread or adding external elements. RepRap BCN 3D+ printer has a screen menu that allows user to stop or pause printing process with a randomly delay. For this application Cura<sup>11</sup> software allows designer to program pauses during printing process and user do not have to watch it.

STOP PRINTING is an extraordinary trick only allowed in the open printers. The utility of this method depends only on the imagination of the user. This study has tested STOP PRINTING for the next cases:

- Repair parts. When user realizes some deformation or unsteady interference, it is recommended to stop printing and solve it manually.
- Horizontal cantilever. TREE method has justified a 66° maximum printing angle. If 90° is required without support material, the methodology is to stop printing and introduce an extra bed, aligned to layer level.
- Screwing. This method can be used to insert a screw during printing and it will be embedded into the 3D printed part.
- Change material. This performance is not tested in this study, but it could be interesting for different material parts with one-extruder printers. However for multi material printing the recommended option is to use a double extruder.

During printing pause extruder is still flowing material and user have to check extruder before restart printing. **CAUTION, use a hand protection to remove added material.**

## **8.7 Lattice 3D honeycomb**

The Infill tests have been an interesting stage for the evaluation of the mechanical properties of the 3D printed parts. Available infill algorithms generate walls of the selected pattern, like an extrusion of the pattern. UAV application is weight restrictive, therefore the effort of this study has been focused on it by developing a lightweight infill.

---

<sup>11</sup> Cura is an open source ULTIMAKER software <https://www.ultimaker.com/pages/our-software>

Lattice 3D structure has been designed with CAD software in a honeycomb pattern. It is the same that a honeycomb infill, but with a lattice 3D structure instead of walls. This is a specific infill for lightweight elements, see Figure 27.

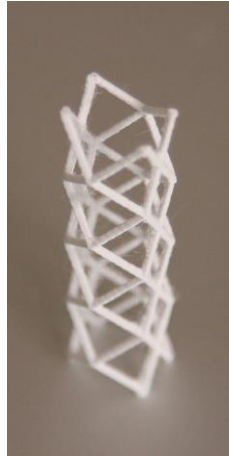


*Figure 27: Lattice 3D honeycomb*

## **8.8 Airfoil**

The most complex part of the UAV to become 3D printed is the airfoil. Its main requirement is the accuracy, in order to manufacture the same airfoil as designed.

Starting from data file, the first step is CAD software importation and extrusion to create the STL file. 3D Printing airfoil has been orientated in the Z printer axis for the Y body axis, see Figure 28, reasons have been the planar basement and the layered smooth aligned to airstream.

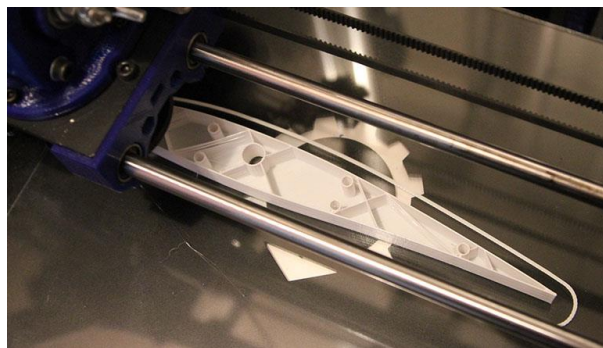


*Figure 28: Airfoil test 3D printing*

### **8.9 Maximum Z axis printing**

The 200mm maximum Z printing size has been tested, see Figure 29, in order to know its performance. This is interesting because UAV will have to be 3D printed by parts and parts number depends on the maximum Z axis available.

Reprap BCN 3D+ has a problem with the filament coil of PLA, not for ABS and NYLON, when extruder is near maximum height. The reason is PLA stiffness that produces interference between extruder movement and coil fixation. This bad performance is increased in the last coil zone where rolled PLA has the minimum diameter.

First large parts 3D printing tests were wrong when extruder stepper could not absorb the filament since it was not aligned to the printer Z axis.

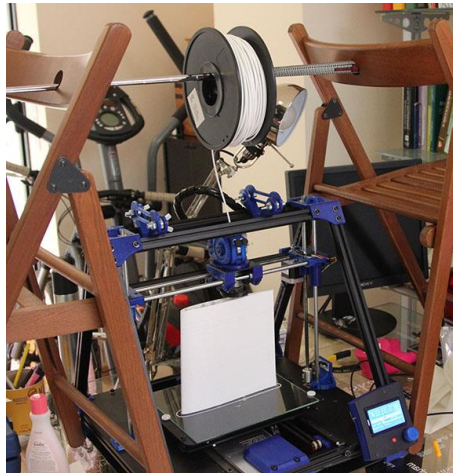


*Figure 29: 200mm Z axis test*

The solution proposed in this study has been to use a top and homemade support for PLA coils using two chairs and a golf club. This recommended modification requires free movement and turn of the coil and extra Z axis distance, near 100mm, from original position. The other important feature when printing large parts is the bed fixation, see 8.1.

## 9 CONCLUSIONS

This document shows that skilled 3D printing designer must control 3D printing configuration parameters.

STL files require a specific method to export wing parts because of the airfoil and wing surfaces complexity.

G-Code is the key configuration for lightweight parts, the interest of this study.

New 3D printing methods, developed in this study, are required for non-support material performance. TREE method is a mandatory rule for the success of the printing process, CHEDDAR method allows to save material, thereby weight and cost reduction, CLICK method is specific for printing mobile and fix parts together and STOP PRINTING allows the user to repair or modify parts during printing process.

The best lightweight performance is a high speed printing with maximum Z axis height and minimum flow of the extruder. All this values according to a functional requirement.

Based on this document, this study is able to design and 3D print a complete UAV.

<b>Prepared by:</b> <b>Jonatan Domènech</b>	<b>Revised by:</b> <b>Pau Nualart Nieto</b> <b>Dra. Jasmina Casals Terré</b>	<b>Study acceptance by:</b> <b>Daniel Garcia Almiñana</b>
--	--	--

Santpedor  
June 2<sup>th</sup>, 2014

## 4 REFERENCES

- [1] RepRap, "Home | RepRapBCN." [Online]. Available: <http://www.reprapbcn.com/>. [Accessed: 26-May-2014].
- [2] M. Nikzad, S. H. Masood, and I. Sbarski, "Thermo-mechanical properties of a highly filled polymeric composites for Fused Deposition Modeling," *Mater. Des.*, vol. 32, pp. 3448–3456, 2011.
- [3] E. plastic trade Association, "PlasticsEurope - Acrylonitrile-Butadiene-Styrene (ABS) - PlasticsEurope." [Online]. Available: <http://www.plasticseurope.org/what-is-plastic/types-of-plastics-11148/engineering-plastics/abs.aspx>. [Accessed: 26-May-2014].
- [4] N. Mediati, "3D PRINTING.," *PC World*, vol. 31, p. 67, 2013.
- [5] E. plastic trade Association, "PlasticsEurope - Bio-based plastics - PlasticsEurope." [Online]. Available: <http://www.plasticseurope.org/what-is-plastic/types-of-plastics-11148/bio-based-plastics.aspx>. [Accessed: 26-May-2014].
- [6] C. Bastioli, *Handbook of Biodegradable Polymers*, vol. 128. 2011, p. 1001.
- [7] K. F. . J. Schoch, "NYLON PLASTICS HANDBOOK," *IEEE Electr. Insul. Mag.*, vol. 12, 1996.
- [8] S. Murase, A. Inoue, Y. Miyashita, N. Kimura, and Y. Nishio, "Structural characteristics and moisture sorption behavior of nylon-6/clay hybrid films," *J. Polym. Sci. Part B Polym. Phys.*, vol. 40, pp. 479–487, 2002.
- [9] ASTM, "ASTM D638 - 10 Standard Test Method for Tensile Properties of Plastics." [Online]. Available: <http://www.astm.org/Standards/D638.htm>. [Accessed: 27-May-2014].
- [10] P. Gruber and M. O'Brien, "Polylactides 'Natureworks® PLA,'" *Biopolym. Online*, pp. 235–239, 2002.
- [11] M. Szilvsi-Nagy and G. Mátyási, "Analysis of STL files," *Mathematical and Computer Modelling*, vol. 38. pp. 945–960, 2003.

- [12] M. Kovacic, M. Brezocnik, I. Pahole, J. Balic, and B. Kecelj, "Evolutionary programming of CNC machines," *J. Mater. Process. Technol.*, vol. 164–165, pp. 1379–1387, 2005.
- [13] Slic3r, "Slic3r Manual - Infill Patterns and Density." [Online]. Available: <http://manual.slic3r.org/expert-mode/infill.html>. [Accessed: 27-May-2014].
- [14] A. C. Rencher and G. B. Schaalje, *Linear Models in Statistics*. 2007, pp. 1–672.
- [15] ULTIMAKER, "Our printers - Ultimaker 2 - Ultimaker." [Online]. Available: <https://www.ultimaker.com/pages/our-printers/ultimaker-2>. [Accessed: 27-May-2014].
- [16] C. RepRap, "Forums | RepRapBCN." [Online]. Available: <http://www.reprapbcn.com/es/forum>. [Accessed: 27-May-2014].
- [17] F. M. White, *Fluid Mechanics*, vol. 17. 2009, p. 864.